Hindawi Publishing Corporation
Advances in Mechanical Engineering
Volume 2013, Article ID 801964, 10 pages
http://dx.doi.org/10.1155/2013/801964

Research Article

Melt Pressure Signature Tracking Using an Adaptive Kalman Filter in Microinjection Molding

Hang Liu,[1] Hong Hu,[1] Kai Leung Yung,[2] Yan Xu,[2] and Xing Wei Zhang[3]

[1] *Harbin Institute of Technology Shenzhen Graduate School, Shenzhen 518055, China*
[2] *Department of Industrial & Systems Engineering, The Hong Kong Polytechnic University, Hung Hom, Kowloon, Hong Kong*
[3] *College of Engineering Shantou University, Shantou University, Shantou 515063, China*

Correspondence should be addressed to Hong Hu; honghu@hit.edu.cn

Received 13 May 2013; Accepted 23 July 2013

Academic Editor: Lei Zhang

In order to manufacture high quality microproducts, the precision control of injected plastic melt in the injection chamber during a microinjection process requires real-time tracking of the melt pressure when the melt passes through the nozzle. A novel type of adaptive Kalman filter algorithm based on F-distribution is proposed in this paper. This adaptive Kalman filter can switch the system between the steady state and transient state by comparing the differences of input data in F-distribution. By resetting the Kalman gain and other relevant parameters, the adaptive function guarantees the convergence of the filtered signal during the tracking process and tracks the moments which sudden changes occur in the pressure signature. The simulation experiment results show that the method can reduce the effect of measurement noise more quickly and effectively. The method is proven to be effective for microinjection molding applications.

1. Introduction

Target tracking, which is considered to be a problem caused by the uncertainty of the target's acceleration, has been studied in the field of state estimation for decades. In micro injection molding, the tracking of the target's acceleration is very important for shot volume control. The micro injection molding process heats plastic granules to melting point and then injects a precise amount at high pressure through a nozzle into a mold. Micro injection has many merits and is one of the most cost effective methods in the mass production of components. It has a stable quality and good dimensional accuracy down to a micrometer. Due to the high sensitivity of the microstructures, a very precise volume of plastic melt is required. In order to achieve high precision volume control, a micro injection machine has been developed in our lab, a sketch of which is shown in Figure 1. The injection unit has a nozzle at its end that connects to the mold, and the plunger can push the molten plastic which passes through the nozzle into the mold. A pressure sensor is mounted in the injection unit for monitoring the micro injection process and promoting the precision of the volume control.

Since the electromagnetic noise severely hinders recognition of the pressure (sharp increment) signature in the micro injection process, a pressure signal process is required. The Kalman filter has been widely used as a tracking filter to estimate the position, the velocity, and the acceleration of a target. Most digital tracking filters are based on the Kalman filter equations, where the process noise and the measurement noise are presumed white. In the most simple models, target accelerations or acceleration increments are regarded as white noise, as is done to obtain the well-known α-β (-γ) filters. These basic discrete-time filters have properties suitable for many applications [1]. The least-mean-square (LMS) algorithm and the recursive least-squares (RLS) algorithms have established themselves as the principal tools for linear adaptive filtering. Lopes and Gerald used the LMS algorithm to get the faster convergence and a much higher noise immunity when the reference signal vector norm takes on a low value [2], while Barnawi et al. used RLS algorithm

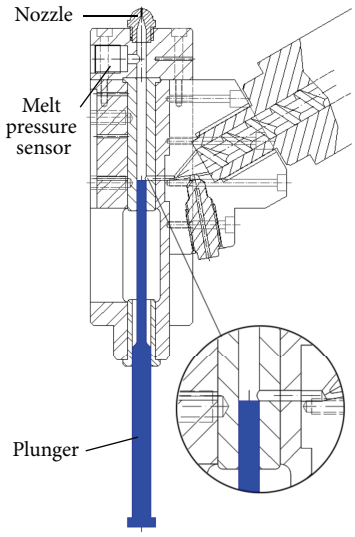

Figure 1: Sketch of injection unit.

to get much less convergence time [3]. Rosendo Macías and Expósito presented a method for self-tuning of the model error covariance to overcome the sudden changes of the input signal, so that they could properly track signal fluctuations in digital protection applications [4]. In the similar field, Hu et al. [5] developed the new adaptive Kalman algorithm which has a good robustness and can handle the sudden changes of vehicle motion and measurement errors. Lee et al. [6] proposed the interacting multiple model algorithm using intelligent input estimation for maneuvering target tracking. Anilkumar et al. utilized the constant Kalman gains for an efficient online prediction of the reentry time of space objects [7]. J.-Y. Kim and T.-Y. Kim proposed the dynamic Kalman filter which robustly tracks a ball in the dynamic condition by controlling the velocity of the state vector [8]. Based on the ARMA innovation model and Lyapunov equations, Deng et al. [9] presented an approach to handle the information fusion filtering, prediction, and smoothing problems for the state and signal. Ding et al. [10] and Geng and Wang [11] proposed the adaptive Kalman methods to tune the Q matrix to the optimal magnitude automatically. Geng and Wang [11] used the statistical method of Chi-square test to evaluate the filter residuals.

Concluding the above methods, the recursive algorithm based on analysis, as given by the Kalman filter, is a good way to detect abrupt changes (transients) of harmonic parameters. Micro injection molding is a fast procedure, but it needs a real-time tracking filter to deal with the abrupt changes during the procedure. From the above methods, in order to deal with the abrupt changes, we consider that developing an adaptive Kalman filter to track the micro injection molding procedure is suitable. The method is easy and robust.

This research proposes a novel adaptive Kalman filter that tracks the pressure signature's sudden change around the nozzle during the micro injection molding process. Simulation results show that this new method accurately tracks the pressure signal profile in high and low speed injection and that its processed pressure signature is consistent with design standards.

2. Methods of Signature Filtering

2.1. Problems. During the micro injection procedure, the injection volume control is of great importance. The control method needs correct and real-time signals. The signals are always acquired by a pressure sensor and processed by a tracking filter. The micro injection procedure is divided into two stages: uniform injection and deceleration injection. Before the plastic melt reaches the nozzle position, the ascending plunger pushes the molten melt at a uniform speed. This is the preinjection stage. When the plastic melt front passes the nozzle, the pressure sensor will catch the melt arrival signal. Then the signal should be transferred to the computer and processed by the real filter. Based on the filtered signal, the melt's arrival instant should be ascertained. The shooting controller will then adjust the shooting parameters and feedback to the linear motor. The plunger first maintains its travelling speed for a finite instant, then gradually slows down to zero. That is the injection stage.

During the micro injection procedure, the signal generated by the plastic melt passing through the nozzle is called the pressure signature. If a tracking filter is not used to deal with the pressure signature, the electromagnetic noise in the pressure signature may cause an error of judgment on the micro injection control unit, which means that the injection volume may be less or more than the volume needed. This may cause insufficient and excessive shootings. Figure 2 and Figure 3 show insufficient and excessive shootings during the micro injection molding procedure, without a real-time tracking filter.

2.2. Kalman Filter Process. The Kalman filter is a set of mathematical equations that provide an efficient computational (recursive) solution to the discrete data linear filtering problem [12]. The Kalman filter addresses the general problem of trying to estimate the state $x \in R^n$ of a discrete-time controlled process that is governed by the linear stochastic difference equation:

$$x_k = Ax_{k-1} + Bu_{k-1} + w_{k-1}, \tag{1}$$

with a measurement $z \in R^m$; that is,

$$z_k = Hx_k + v_k, \tag{2}$$

where u is the control input. A is the $n \times n$ matrix that relates the state at the previous time step to the current step. B is the $n \times 1$ matrix that relates the control input. H is the $m \times n$ matrix that relates the state. The random variables w_k and v_k represent the process and measurement noise, respectively.

The final estimation algorithm is the predictor corrector for solving numerical problems. The discrete Kalman filter time update equations are the following.

(1) Project the state ahead:

$$\widehat{x}_k^- = A_k\widehat{x}_{k-1} + B_k u_k, \tag{3}$$

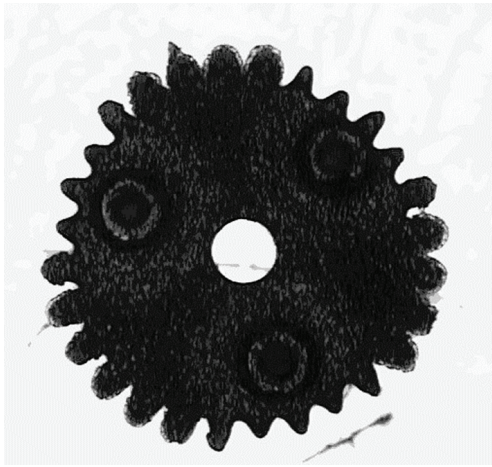

Figure 2: Insufficient shooting.

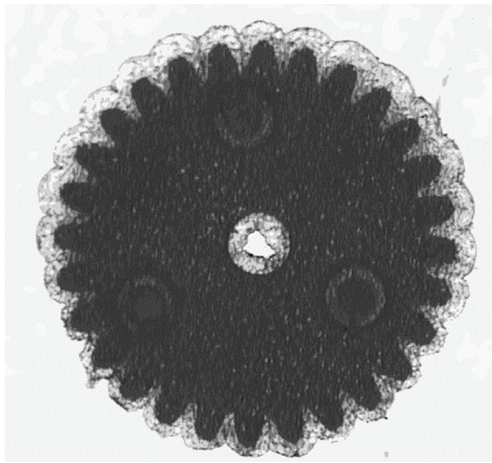

Figure 3: Excessive shooting.

(2) project the error covariance ahead:

$$P_k^- = A_k P_{k-1} A_k^T + Q. \tag{4}$$

The discrete Kalman filter measurement updates equations:

(1) compute the Kalman gain:

$$K_k = P_k^- H^T \left(H P_k^- H^T + R \right)^{-1}, \tag{5}$$

(2) update estimate with measurement:

$$\widehat{x}_k = \widehat{x}_k^- + K_k \left(z_k - H \widehat{x}_k^- \right), \tag{6}$$

(3) update the error covariance:

$$P_k = \left(I - K_k H \right) P_k^-, \tag{7}$$

where Q is the process noise covariance and the elementary matrix, R is the measurement noise covariance, $\widehat{x}_k^-$ is the a priori state estimate, $\widehat{x}_k$ is the a posteriori state estimate, P_k^- is the a priori estimate error covariance, P_k is the a posteriori estimate error covariance, K_k is the Kalman gain, R is the measurement error covariance, and H is the $m \times n$ matrix that relates the state to the measurement.

After each time and measurement update, the process is repeated with the previous a posteriori estimates used to project or predict the new a priori estimates. This recursive nature will timely adjust itself and track the varying signature acquired. It is also easy to use mathematical induction to prove the correctness of the algorithm [13].

2.3. Adaptive Kalman Filter Based on F-Distribution. Although the Kalman filter provides a dynamic and precise parameter estimation of the injection process, it often suffers from a problem known as "filter dropping off." That is, if the parameters to be estimated have not been changed for a long time, the filter parameters (Kalman gain K, internal error covariance matrix P) have a very small stationary value, and the filter becomes insensitive to abrupt changes of state variables. Thus, in the case of the estimation of dynamic variations of signature components, the standard Kalman filter loses the ability to match these changes quickly. A previous study [14] of the adaptive Kalman filter focused on the t-distribution to distinguish the two different models for steady-state and transient-state estimations. However, due to its poor robustness, the Kalman filter based on the t-distribution can be only used in low speed and low noise injection molding environments because it is not able to track the pressure signature and causes mistakes at higher injection velocities. For a wider application of injection molding requirements, the adaptive Kalman filter based on F-distribution is proposed. A hypothesis-testing procedure for the equality of two variances is based on the following procedure. Let $\{X_{11}, X_{12}, \ldots, X_{1x}\}$ be a random sample from a normal population with variance σ_1^2, and then let $\{X_{21}, X_{21}, \ldots, X_{2y}\}$ be a random sample from a second normal population with variance σ_2^2. Assume that both normal populations are independent. Let S_1^2 and S_2^2 be the sample variances. Then the ratio is

$$F = \frac{S_1^2}{S_2^2}, \tag{8}$$

where the F-distribution has $x - 1$ degrees of freedom at the numerator and $y - 1$ degrees of freedom at the denominator.

The steps are as follows.

Firstly get n pressure data from the recent pressure signature, assuming the data group as $\{X_1, X_2, \ldots, X_n\}$ and the variance of the data group is σ_x. Secondly, erase the first data X_1 and add the current data X_{n+1} at the next sample time, so the current data group becomes $\{X_2, X_3, \ldots, X_{n+1}\}$ and the variance of the data group is σ_y.

The null hypothesis $H_0 : \sigma_x^2 = \sigma_y^2$, alternative hypothesis $H_1 : \sigma_x^2 \neq \sigma_y^2$, and rejection criterion is $F_0 > F_{\alpha/2,x-1,y-1}$ or $F_0 < F_{1-\alpha/2,x-1,y-1}$. Assume $\alpha = 0.05$ (the value of α is decided by analyzing the data and is changeable); if the value of F is within the significance of $\alpha = 5\%$, it means that

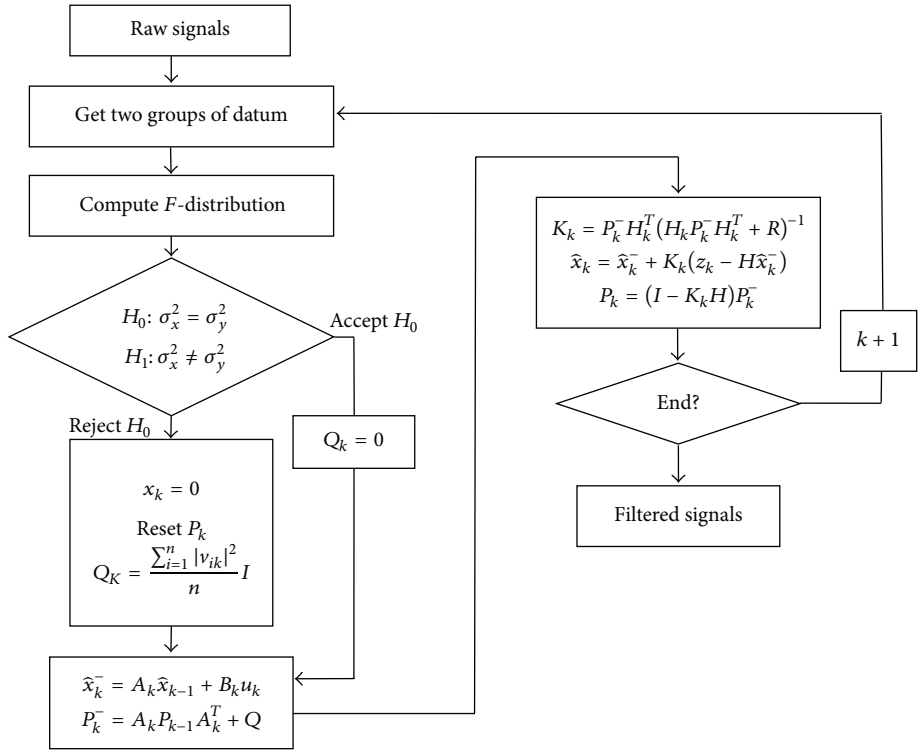

Figure 4: Adaptive Kalman filter based on F-distribution flow chart.

the current pressure signature is in the steady state, and the traditional Kalman process from (3) to (7) can be used to filter the pressure signals. If the value of F is out of the significance of $\alpha = 5\%$, it means that the current pressure signature is in the transient state; then from (2) we get

$$v_k = z_k - H_k x_k, \tag{9}$$

where v_k is the filter error and the input x_k resets as zero; thus, v_k is equal to z_k. At this time, the value of P_k in (7) is becoming smaller because of the long time steady-state estimation, so a larger value of P_k is required to increase the Kalman gain K_k for transient-state estimation. The new $\hat{x}_k$ in (6) from the changed K_k is best fit for the transient-state estimation. Meanwhile, as the value of the noise Q_k in (4) is becoming smaller and will not fit the transient situation, the model sets a lower value for it. When the transient estimation is coming, the Q_k will be reset as

$$Q_k = \frac{\sum_{i=1}^{n} |v_{ik}|^2}{n} I, \tag{10}$$

where n is the order for the model and I is the identity matrix [4]. So the adaptive Kalman filter consists of steady and transient estimations by using the F-distribution judgment, where the steady estimation performs the traditional Kalman filter, and the transient estimation performs parameter resets and the traditional Kalman filter. The computational sequence for the adaptive Kalman filter is shown in Figure 4.

For an adaptive Kalman filter, when $k \to \infty$ and $K_k \to 0$, the filter is divergent with an increasing k value. We can prove that K_k is always greater than zero and the stability of the adaptive Kalman filter. During micro injection, if the null hypothesis is accepted, it means that the melt front has not yet reached the nozzle and the system is assumed to be in a steady state ensuring Q_k to be 0. Likewise, if the null hypothesis is rejected, it means that the plastic melt front reaches the nozzle and the system is assumed to be in a transient state and resets to a set of initial conditions. Suppose when $k \to \infty$, $K_k \to 0$, from (2), we can get

$$K_k = P_k^- H_k^T \left(H_k P_k^- H_k^T + R_k\right)^{-1}. \tag{11}$$

Because H_k and R_k are not zero, $P_k = 0$:

$$\begin{aligned} P_{k+1}^- &= A_k P_k A_k^T + Q_k = Q_k > 0, \\ P_k &= \left(I - K_k H_k\right) P_k^- = P_k^- > 0. \end{aligned} \tag{12}$$

This clearly contradicts the conclusion of $P_k = 0$. So $K_k > 0$, and the filter is not divergent. The adaptive Kalman filter based on F-distribution can track real-time signal and perfectly overcome the "filter dropping off" problem. Compared with the Kalman filter, the robustness of the adaptive Kalman filter based on F-distribution makes it suitable for many more injection molding purposes. In view of the above, this adaptive Kalman filter based on F-distribution uses the statistical methods to adjust the system's state. The Q model will be replaced if the system's state is changed from steady to transient. It avoids the search time of the optimal Q in original Kalman filter, so it meets the real time needs in micro injection molding procedure.

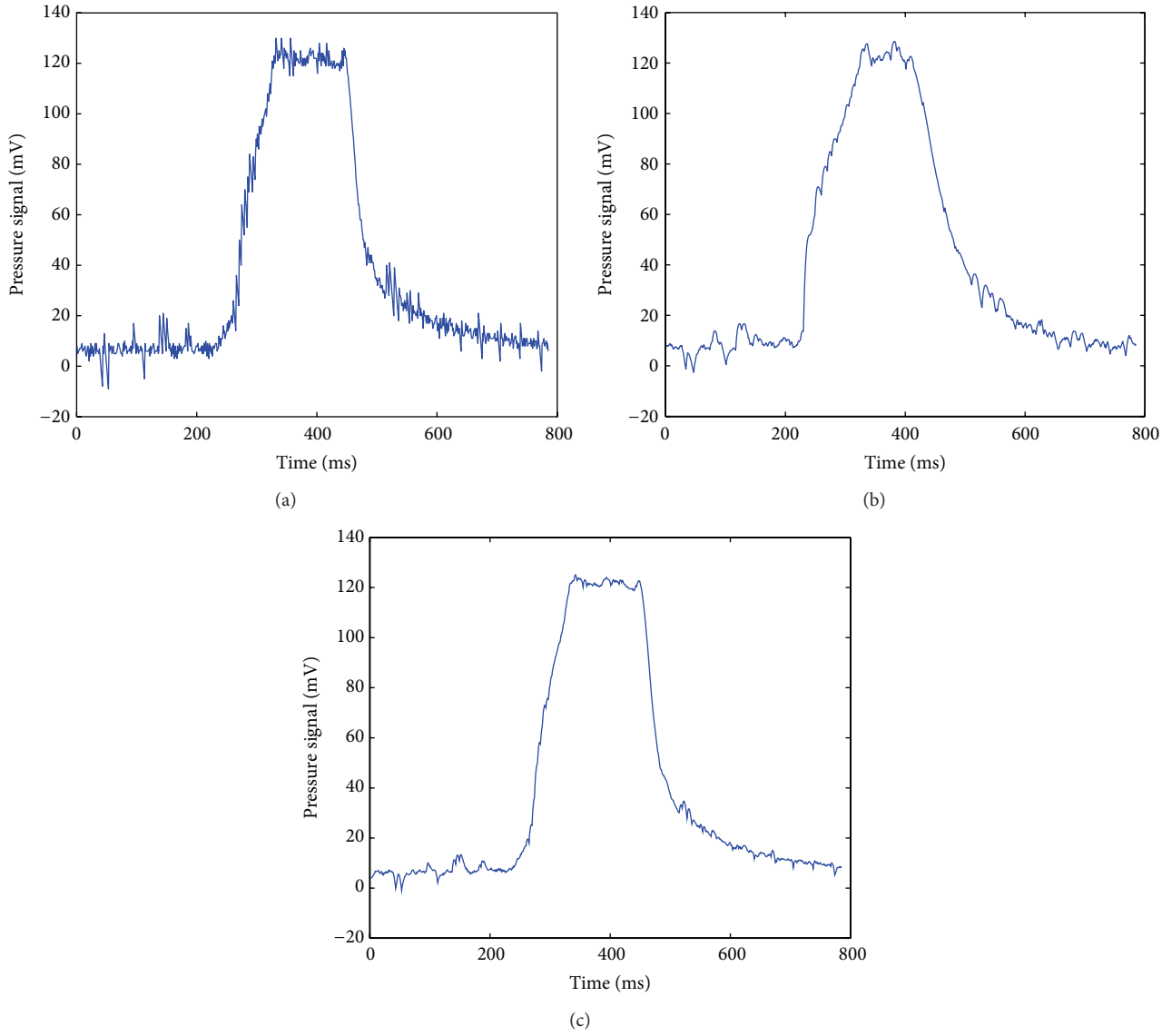

FIGURE 5: Injection velocity 50 mm/s. Signature width 340 ms. Signature peak height 125 mV. Injection volume 0.12 cc. (a) Experimental pressure signature without filter. (b) Experimental pressure signature processed by traditional Kalman filter. (c) Experimental pressure signature processed by adaptive Kalman filter based on F-distribution.

3. Simulation Comparison

To realize accurate injection volume control of plastic melt during micro injection, the effective detection of the moment for the arrival of the plastic melt front at the injection nozzle is necessary. The plastic PMMA (MF-001) is selected for the pressure signature tracking in our micro injection experiments. The temperature of the injection part is 240°C. The diameter of the nozzle is 2.0 mm and made of stainless steel. Due to the high injection velocity associated with the micro injection machine, the pressure sensor responsible for monitoring the nozzle pressure requires a high sensitivity and frequency response. A piezoelectric melt pressure sensor manufactured by Kistler is employed and is mounted beneath the nozzle (Kistler 6171BA, range = 0 to 2000 bar). The plastic melt generates the pressure signature during its passage through the nozzle (Figure 1). Before the plastic melt reaches the tapered nozzle, the pressure change recorded by the pressure sensor would be minor. Yet, when the plastic melt flows through the narrowed opening at a constant volume flow rate (depends on the traveling speed of the plunger), the developed pressure causes the signal to undergo a sudden rise and maintains its maximum level for a finite instant; then the signature performs a rapid decline as the plunger stops at its end position. The purpose of the current study is to investigate the role of the difference in filtering the pressure signatures between the traditional Kalman filter and adaptive Kalman filter based on F-distribution. Different injection

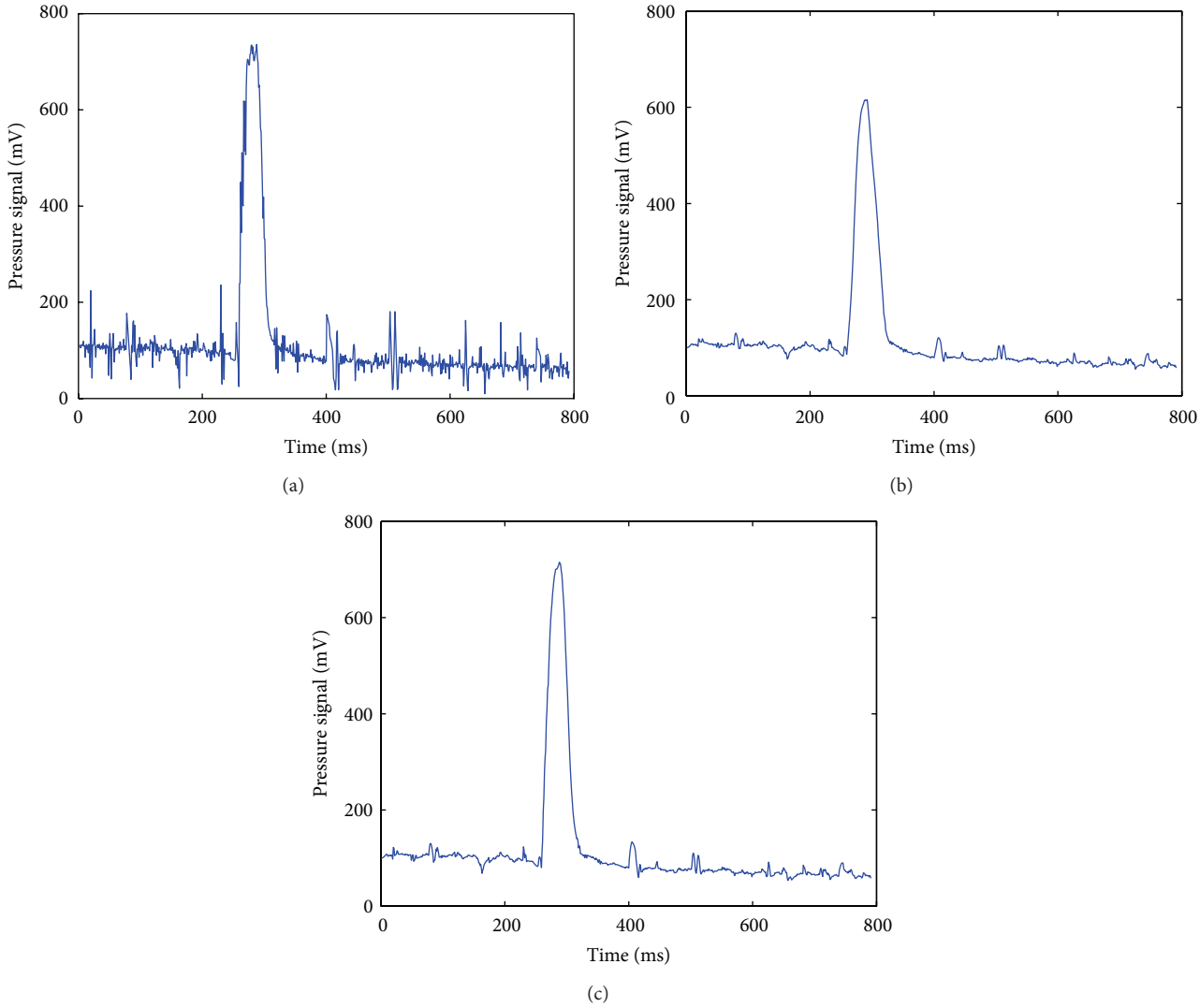

Figure 6: Injection velocity 475 mm/s. Original signature width 60 ms. Signature peak height 624 mV. Injection volume 0.12 cc. (a) Experimental pressure signature without filter. (b) Experimental pressure signature processed by traditional Kalman filter. (c) Experimental pressure signature processed by adaptive Kalman filter based on F-distribution.

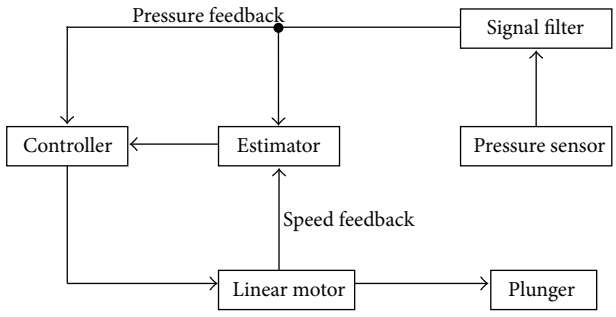

Figure 7: Signal process flow chart.

velocities are selected to compare the pressure signatures filtered by the traditional Kalman filter and the adaptive Kalman filter based on F-distribution.

The pressure signatures under different injection velocities are obtained by a pressure sensor (Kistler 6171BA, range = 0 to 2000 bar) and plotted by MATLAB 7; then the signatures are processed by MATLAB 7 using the traditional Kalman filter and adaptive Kalman filter based on F-distribution, respectively. The simulation results are shown in Figures 5 and 6. The simulation computer's CPU is Intel Core i7-2620M Dual-Core Processor. The memory is 8 GB DDR3 1333 MHz. In Figure 5 the injection velocity is 50 mm/s, the signature width is 342 ms, the signature peak height is 125 mV, and the injection volume is 0.12 cc. In Figure 6 the injection velocity is 475 mm/s, the original signature width is 60 ms, the signature peak height is 624 mV, and the injection volume is also 0.12 cc. Figures 5(a) and 6(a) show the experimental pressure signatures without filter. We can see the signatures have severe electromagnetic noise; this may affect the judgment of the start and end points during the micro injection procedure.

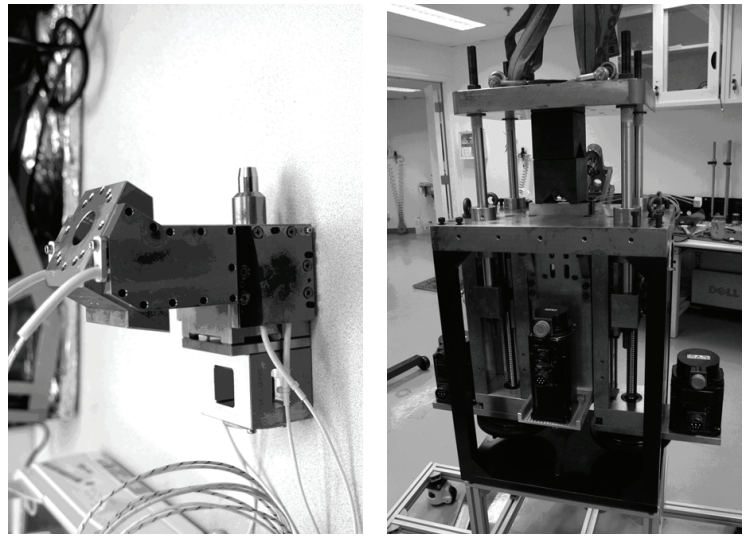

(a) (b)

Figure 8: (a) Injection part. (b) Micro injection molding machine.

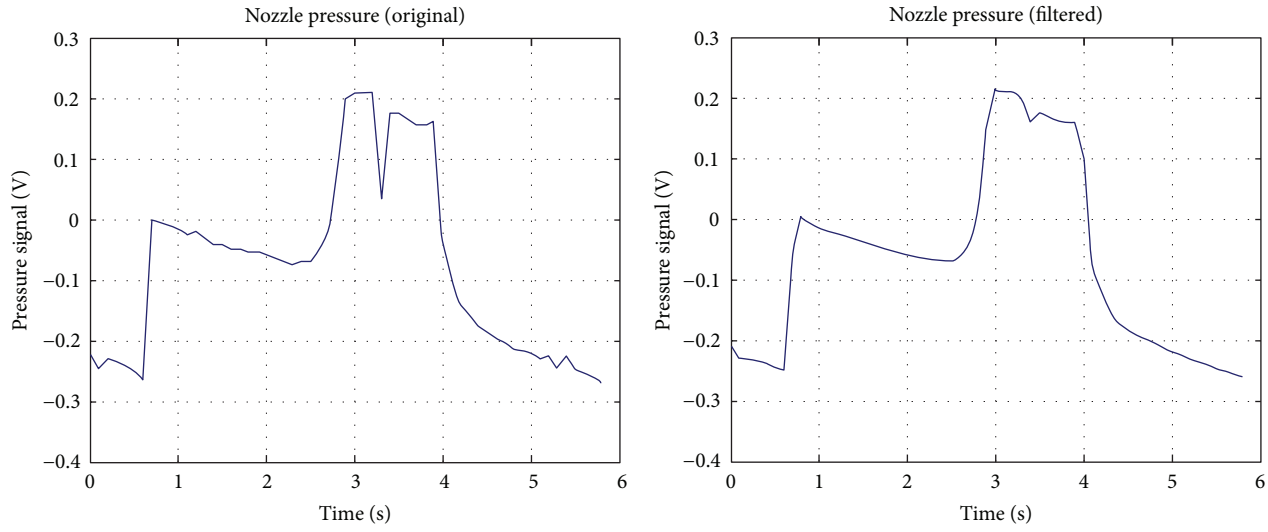

(a) (b)

Figure 9: Experiment plastic POM. Injection velocity 15 mm/s. Injection volume 0.32 cc. (a) Original signature: signature width 3350 ms, signature peak height 445 mV. (b) Filtered signature: signature width 3356 ms, signature peak height 443 mV.

Figures 5(b) and 6(b) show the experimental pressure signatures processed by traditional Kalman filter. In Figure 6(b), the peak height of pressure signature is lower than that in Figure 6 (a), which only has got 530 mV, while in Figures 5(b) and 6(b), the pressure signatures have longer rising edges and falling edges because of the "filter dropping off," so the signature widths of Figures 5(b) and 6(b) are 450 ms and 84 ms, respectively. They are longer than the signature widths in Figures 5(a) and 6(a), which may cause excessive shooting (Figure 3). From Figures 5(c) and 6(c), we can see the pressure signatures processed by adaptive Kalman filter based on F-distribution do not have the shortcoming of the traditional Kalman filter. Compared with Figures 5(a) and 6(a), the electromagnetic noise in Figures 5(c) and 6(c) is reduced significantly. The signature widths in Figures 5(c) and 6(c) are 346 ms and 62 ms, and the signature peak heights are still the same as the original signatures. From the simulation results we can see the adaptive Kalman filter based on F-distribution performs better in the micro injection molding procedure.

4. Experiments

The injection volume control needs to get the precise signature width to confirm when the injection process starts and finishes. From the former simulation results, the adaptive Kalman filter based on F-distribution meets this demand. Then the experiments should be carried out to verify if the adaptive Kalman filter based on F-distribution is suitable

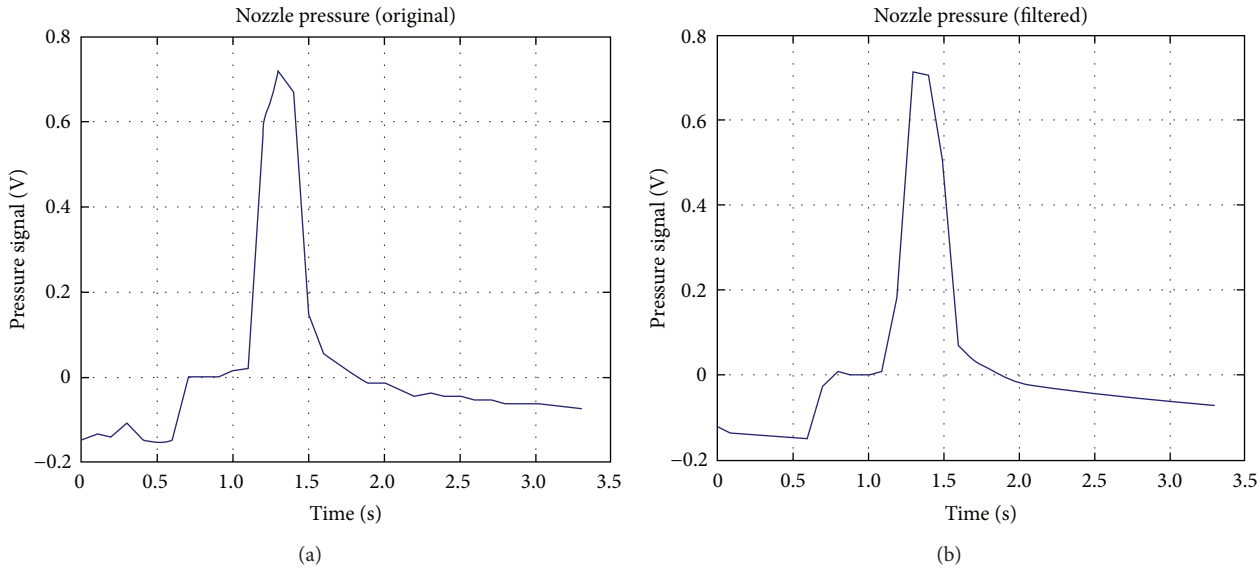

Figure 10: Experiment plastic POM. Injection velocity 150 mm/s. Injection volume 0.45 cc. (a) Original signature: signature width 486 ms, signature peak height 710 mV. (b) Filtered signature: signature width 488 ms, signature peak height 708 mV.

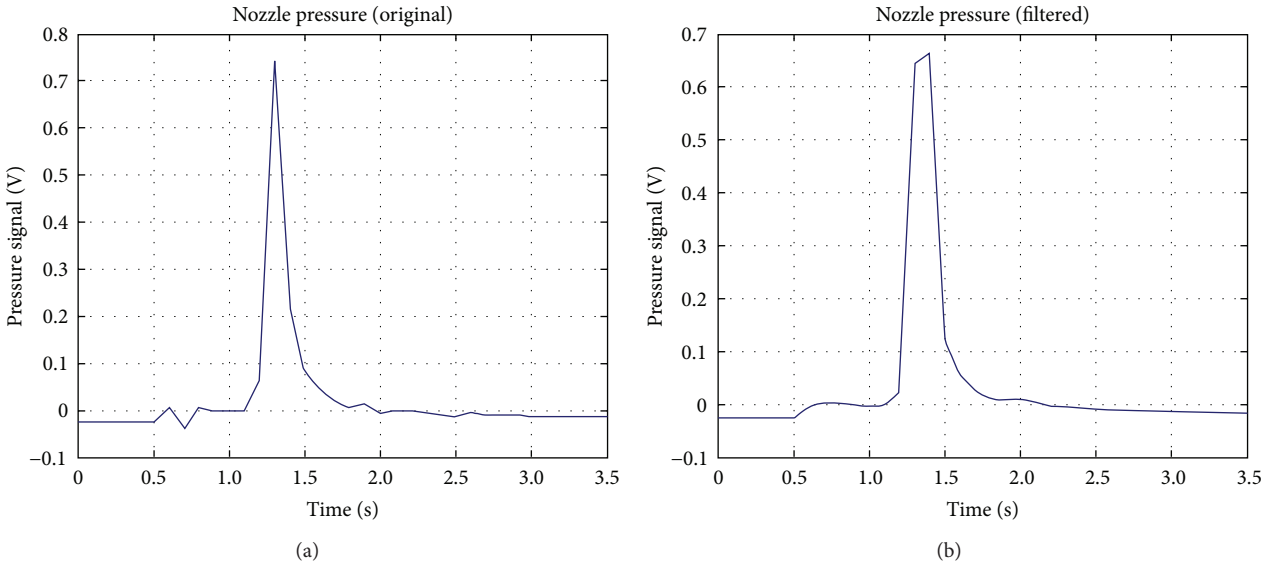

Figure 11: Experiment plastic PMMA. Injection velocity 150 mm/s. Injection volume 0.45 cc. (a) Original signature: signature width 477 ms, signature peak height 753 mV. (b) Filtered signature: signature width 480 ms, signature peak height 768 mV.

for tracking the pressure signature during micro injection molding process.

Figure 7 shows the signal process flow chart for the micro injection molding procedure. The controller and the estimator are called the control part. The pressure signal filter is called the pressure feedback. The control part uses the pressure feedback and the speed feedback to adjust the travelling speed of the plunger. So it is very important to get the correct and real-time pressure signatures from the digital filter.

A series of experiments is conducted to study the effects of plastic material when using the adaptive Kalman filter based on F-distribution. The rejection criterion α is chosen as 5% by analyzing the experiments' results. The injection assembly and the assembly of the micro injection molding machine are shown in Figures 8(a) and 8(b). The pressure sensor is the Kistler 6171BA (range = 0 to 2000 bar). The sensor is in turn connected to a charge amplifier (Kistler 5039A, range = 0 to 20,000 pC), which converts the charge generated by the sensor to a voltage that represents the measured pressure. The oscilloscope is Tektronix TDS 3014B and the control theory is proportional-integral-derivative (PID) control.

In the injection experiments we have recorded the original and the filtered pressure signatures. Figures 9, 10, and 11 depict the injection process with different shot volumes at

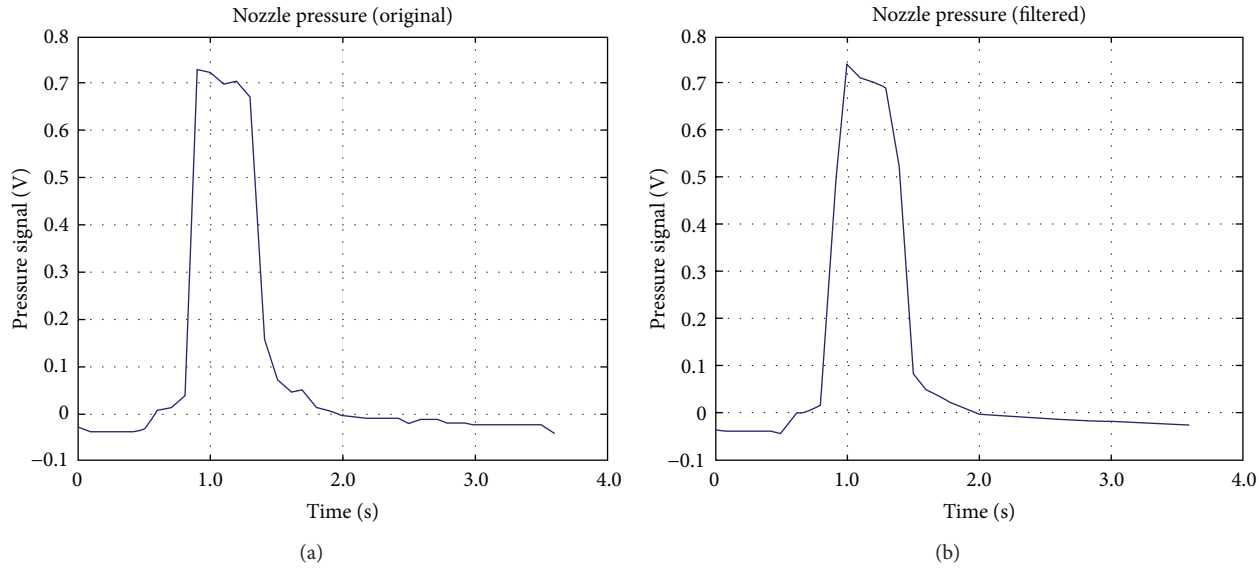

Figure 12: Microgear trial production. Experiment plastic POM. Injection velocity 150 mm/s. Injection volume 0.86 cc. (a) Original signature: signature width 989 ms, signature peak height 696 mV. (b) Filtered signature: signature width 993 ms, Signature peak height 695 mV.

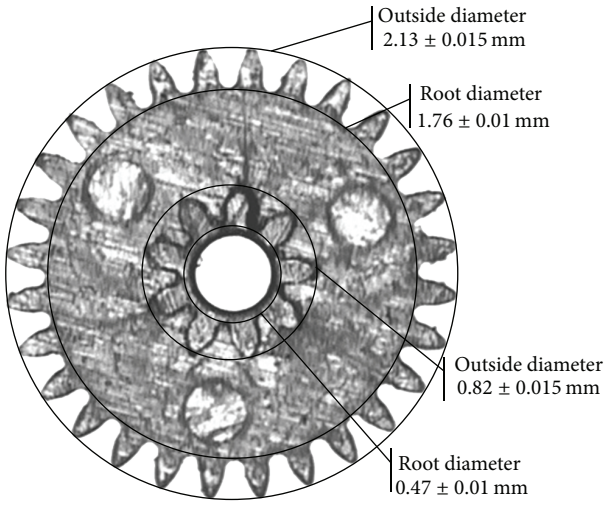

Figure 13: Micro gear profile and some of the dimension demands.

different injection velocities by using different plastics. The plastic POM (Delrin 900P) is used in Figures 9 and 10. The plastic PMMA (MF-001) is used in Figure 11. In Figure 9, the injection velocity is 15 mm/s, and the injection volume is 0.32 cc. Figure 9(a) shows that the original signature width is 3350 ms and the signature peak height is 445 mV. Figure 9(b) shows the filtered signature width as being 3356 ms with a signature peak height of 443 mV. In Figure 10, the injection velocity is 150 mm/s and the injection volume is 0.45 cc. Figure 10(a) depicts the original signature width as 486 ms and the signature peak height as 710 mV. Figure 10(b) shows that the filtered signature width is 488 ms and the signature peak height is 708 mV. In Figure 11, the injection velocity is 150 mm/s and the injection volume is 0.45 cc. Figure 11(a) depicts the original signature width as 477 ms and the signature peak height as 753 mV. Figure 11(b) shows that the filtered signature width is 480 ms and the signature peak height is 768 mV. From the datum it can be seen that the rising edges of the pressure signatures are captured perfectly and the delay times are very short. The changes of peak height between the original and filtered signatures are tiny in Figures 9 and 10, but the change is larger in Figure 11. However, the signature width change between Figures 11(a) and 11(b) is still tiny. So it will not affect the injection volume control. In view of the above, the experimental and simulation results are consistent; no matter how the injection velocity changes, the filtered pressure signatures are always stable and reliable. It is good for the accuracy control of the micro injection molding process. Also, the filter can effectively eliminate the high frequency electromagnetic noise in the pressure transducer signal.

To further test the accuracy and micro injection performance of the new filter, a microgear is produced by the micro injection molding machine. The plastic material used in the experiment is POM (Delrin 900P). As there are 16 microcavities in the mold, 16 microgears can be accessed during the micro injection molding procedure. The pressure signature of the micro gear trial production is shown in Figure 12. The injection velocity is 150 mm/s, and the injection volume is 0.86 cc. Figure 12(a) shows that the original signature width is 989 ms and that the signature peak height is 696 mV. Figure 12(b) shows that the filtered signature width is 993 ms and that the signature peak height is 695 mV. Figure 13 shows the profile of the microgear product used in the experiment and some of its dimension demands. The profile is taken by the Leica DM300 microscope. The microgear has two layers in Figure 13. The outer gear has 28 teeth; the outside diameter is 2.13 ± 0.015 mm, and the root diameter is 1.76 ± 0.01 mm. The inner gear has 9 teeth; the outside diameter is 0.82 ± 0.03 mm, and the root diameter is 0.47 ± 0.03 mm. It

Table 1: Measurement result of outer gear (diameter).

Number	Outside diameter (mm)	Root diameter (mm)
1	2.125	1.752
2	2.126	1.763
3	2.139	1.766
4	2.122	1.769
5	2.132	1.764
6	2.137	1.755
7	2.137	1.753
8	2.131	1.752
9	2.135	1.759
10	2.128	1.752
11	2.125	1.763
12	2.136	1.754
13	2.138	1.754
14	2.131	1.760

Table 2: Measurement result of inner gear (radius).

Number	Outside radius (mm)	Root radius (mm)
1	0.406	0.233
2	0.407	0.234
3	0.407	0.232
4	0.411	0.231
5	0.413	0.237
6	0.410	0.238
7	0.406	0.238
8	0.409	0.231
9	0.417	0.230

has very subtle teeth and a delicate tooth profile. It validates the effectiveness of the filter.

The measurement tool is the Leica DM300 microscope. As the outer gear has an even number of teeth, the opposite two vertexes are measured to determine the diameters; the results are shown in Table 1. The inner gear has an odd number of teeth, so the center of the micro gear is first fixed by two intersecting diameters of the outer gear, and then the radius of the inner gear is measured; the results are shown in Table 2. The dimension demands for radius of the inner gear are adjusted as the outside diameter is 0.41 ± 0.015 mm and the root diameter is 0.235 ± 0.015 mm. From Tables 1 and 2, we can see the measurement data of the micro gear produced satisfies the dimension demands proposed.

5. Conclusion

This paper derives an adaptive Kalman filter based on F-distribution to track the pressure signature generated by an ascending plunger that pushes plastic melt through a nozzle into a micro injection mold. The filter switches the system between a transient and steady state in real time, effectively eliminating electromagnetic noise and precisely capturing the rising and falling edges of the pressure signature. According to the simulation results, the adaptive Kalman filter avoids the shortcoming of the original Kalman filter at high and low injection velocities, and the pressure signatures meet control requirements. The experimental filter satisfies dimension demands and is proven suitable for use in the mass production of micro injection moldings.

Acknowledgments

This work is supported in part by the Hong Kong Innovation & Technology Foundation (ITF/025/03), the Natural Science Foundation of China (NSFC) under Grant 60974069, and Shenzhen Government Foundation under JC200903120188A.

References

[1] B. Ekstrand, "Poles and zeros of α-β and α-β-γ tracking filters," *IEE Proceedings on Control Theory and Applications*, vol. 148, no. 5, pp. 370–376, 2001.

[2] P. A. C. Lopes and J. B. Gerald, "New normalized LMS algorithms based on the Kalman filter," in *Proceedings of the IEEE International Symposium on Circuits and Systems (ISCAS '07)*, pp. 117–120, May 2007.

[3] A. Barnawi, A. Albakkar, and O. P. Malik, "RLS and Kalman Filter identifiers based adaptive SVC controller," in *Proceedings of the 39th North American Power Symposium (NAPS '07)*, pp. 615–622, October 2007.

[4] J. A. Rosendo Macías and A. G. Expósito, "Self-tuning of Kalman filters for harmonic computation," *IEEE Transactions on Power Delivery*, vol. 21, no. 1, pp. 501–503, 2006.

[5] C. Hu, W. Chen, Y. Chen, and D. Liu, "Adaptive Kalman filtering for vehicle navigation," *Journal of Global Positioning Systems*, vol. 2, pp. 42–47, 2003.

[6] B.-J. Lee, J.-B. Park, and Y.-H. Joo, "IMM algorithm using intelligent input estimation for maneuvering target tracking," *IEICE Transactions on Fundamentals of Electronics, Communications and Computer Sciences*, vol. E88-A, no. 5, pp. 1320–1327, 2005.

[7] A. K. Anilkumar, M. R. Ananthasayanam, and P. V. Subba Rao, "A constant gain Kalman filter approach for the prediction of re-entry of risk objects," *Acta Astronautica*, vol. 61, no. 10, pp. 831–839, 2007.

[8] J.-Y. Kim and T.-Y. Kim, "Soccer ball tracking using dynamic kalman filter with velocity control," in *Proceedings of the 6th International Conference on Computer Graphics, Imaging and Visualization (CGIV '09)*, pp. 367–374, August 2009.

[9] Z.-L. Deng, Y. Gao, L. Mao, Y. Li, and G. Hao, "New approach to information fusion steady-state Kalman filtering," *Automatica*, vol. 41, no. 10, pp. 1695–1707, 2005.

[10] W. Ding, J. Wang, C. Rizos, and D. Kinlyside, "Improving adaptive kalman estimation in GPS/INS integration," *Journal of Navigation*, vol. 60, no. 3, pp. 517–529, 2007.

[11] Y. Geng and J. Wang, "Adaptive estimation of multiple fading factors in Kalman filter for navigation applications," *GPS Solutions*, vol. 12, no. 4, pp. 273–279, 2008.

[12] G. Welch and G. Bishop, *An Introduction To the Kalman Filter*, Department of Computer Science, University of North Carolina at Chapel Hill, 1997.

[13] W. W. Hines and D. C. Montgomery, *Probability and Statistics in Engineering and Management Science*, John Wiley and Sons, New York, NY, USA, 1990.

[14] K. L. Yung, H. Liu, Y. Xu et al., "Target tracking in micro injection molding," *Key Engineering Materials*, vol. 364–366, pp. 1292–1295, 2008.